

1 **‘Warm Cover’- Precursory ‘Strong Signals’ hidden in the Middle**
2 **Troposphere for Haze Pollution**

3

4 **Xiangde Xu¹, Wenyue Cai^{1, 2, 3}, Tianliang Zhao⁴, Xinfu Qiu⁵, Wenhui Zhu⁶, Chan Sun¹, Peng Yan⁷,**
5 **Chunzhu Wang⁸, and Fei Ge⁹**

6 ¹State Key Laboratory of Severe Weather (LASW), Chinese Academy of Meteorological Sciences, Beijing,
7 China.

8 ²National Climate Center, China Meteorological Administration, Beijing, China.

9 ³School of Geographical Science, Nanjing University of Information Science and Technology, Nanjing,
10 Jiangsu Province, China.

11 ⁴Key Laboratory for Aerosol-Cloud-Precipitation of China Meteorological Administration, Nanjing
12 University of Information Science and Technology, Nanjing, Jiangsu Province, China.

13 ⁵School of Applied Meteorology, Nanjing University of Information Science and Technology, Nanjing,
14 Jiangsu Province, China.

15 ⁶Beijing Institute of Applied Meteorology, Beijing, China.

16 ⁷Meteorological Observation Center, China Meteorological Administration, Beijing, China.

17 ⁸Training Center, China Meteorological Administration, Beijing, China.

18 ⁹School of Atmospheric Sciences/Plateau Atmosphere and Environment Key Laboratory of Sichuan
19 Province/Joint Laboratory of Climate and Environment Change, Chengdu University of Information
20 Technology, Chengdu, Sichuan Province, China.

21

22

23 **Correspondence:** Wenyue Cai (caiwy@cma.gov.cn) and Tianliang Zhao (tlzhao@nuist.edu.cn)

24

25 **Abstract.** Eastern China (EC), located in the downstream region of Tibetan Plateau (TP), is a large area
26 with frequent haze pollution. In addition to air pollutant emissions, meteorological conditions were a key
27 ‘inducement’ for air pollution episodes. Based on the study of the Great Smog of London in 1952 and haze
28 pollution in EC over recent decades, it is found that the abnormal ‘warm cover’ (air temperature warm
29 anomalies) in the middle troposphere, as a precursory ‘strong signal’, could connect to severe air pollution
30 events. The convection and vertical diffusion in the atmospheric boundary layer (ABL) were suppressed by
31 a relatively stable structure of ‘warm cover’ in the middle troposphere, leading to the ABL height decreases,
32 which was favourable for the accumulation of air pollutants in the ambient atmosphere. The anomalous
33 structure of the troposphere’s ‘warm cover’ not only exist in heavy haze pollution on the daily scale, but
34 also provide seasonal, interannual and interdecadal ‘strong signals’ for frequently occurring regional haze
35 pollution. It is revealed that a close relationship existed between interannual variations of the TP’s heat
36 source and the ‘warm cover’ strong-signal in the middle troposphere over EC. The warming TP could lead
37 to the anomalous ‘warm cover’ in the middle troposphere from the plateau to the downstream EC region
38 and even the entire East Asian region for air pollution.

39

40 **1 Introduction**

41 In China, mainly over the region east of 100° E and south of 40° N (Tie et al., 2009), PM_{2.5} (particulate
42 matter with an aerodynamic diameter equal to or less than 2.5 μm) has become the primary air pollutant in
43 winter (Wang, et al., 2017). Therefore, in September 2013, the Chinese government launched the China's
44 first air pollution control action plan-‘The Airborne Pollution Prevention and Control Action Plan
45 (2013-2017)’ (State Council of the People’s Republic of China, 2013). By 2017, about 64 % of China’s
46 cities are still suffering from air pollution, especially Beijing-Tianjin-Hebei region and surrounding areas
47 (Wang et al., 2019; Miao et al., 2019). Then, in July 2018, the Chinese government launched the second
48 three-year action plan for air pollution control, ‘the blue sky defense plan’, which demonstrates China's
49 firm determination and new measures for air pollution control (State Council of the People’s Republic of
50 China, 2018). After the implementation of air pollution control action plans, air quality in many regions in
51 China has been significantly improved.

52 Anthropogenic pollutant emissions and unfavorable meteorological conditions are commonly regarded

53 as two key factors for air pollution (Ding and Liu, 2014; Yim et al., 2014; Zhang et al., 2015). Air pollutants
54 mainly come from surface emission sources, and most of air pollutants are injected from the surface to the
55 atmosphere through the atmospheric boundary layer (ABL) (Quan et al., 2020). The ABL structures are the
56 key meteorological conditions which influences the formation and maintenance of heavy air pollution
57 episodes (Wang et al., 2015; Cheng et al., 2016; Wang et al., 2016; Tang et al., 2016; Wang et al., 2019).

58 Most of the previous studies focused on exploring the impact on the heavy air pollution in Eastern
59 China (EC) from the meteorological conditions in ABL. However, the thermodynamic and dynamic
60 structures of free troposphere can affect the meteorological conditions in ABL (Cai et al., 2020). The
61 convection and diffusion in the ABL are suppressed by a relatively stable structure in the middle
62 troposphere, leading to the ABL height decreases, which was favourable for the formation and persistence
63 of heavy air pollution (Quan et al., 2013; Wang et al., 2015; Cai et al., 2020).

64 This study investigated whether the thermodynamic structure of the troposphere and its intensity
65 changes can be used as a ‘strong warning signal’ for the changes of $PM_{2.5}$ concentrations in heavy air
66 pollution, and whether this strong signal exists in the time scales of seasonal, interannual and interdecadal
67 changes. In order to explore the interaction between the free troposphere and the ABL and the impact on
68 the heavy air pollution in EC, this study extended the meteorological conditions for heavy air pollution
69 from the boundary layer to the middle troposphere. We identify a precursory ‘strong signals’ hidden in the
70 free troposphere for frequent haze pollution in winter in EC.

71

72 **2 Data and methods**

73 The data used in this study included NCEP/NCAR and ERA-Interim reanalysis data of meteorology, as
74 well as data of surface $PM_{2.5}$ concentration measurement, air temperature observation and L-band sounding,

75 as briefly described as follows:

76 The monthly NCEP/NCAR reanalysis data of meteorology with horizontal resolution of 2.5° of
77 1960-2019 were obtained from the U.S. National Center for Environmental Protection (NCEP,
78 <https://www.esrl.noaa.gov/>).

79 The daily and monthly ERA-Interim reanalysis data of meteorology with horizontal resolution of 0.75°
80 were derived from the European Center for Medium-range Weather Forecasts (ECMWF,
81 <https://www.ecmwf.int/>), including air temperature, geopotential height, humidity, wind field and vertical
82 velocity.

83 The hourly $PM_{2.5}$ concentration data during 2013-2019 were collected from the national air quality
84 monitoring network operated by the Ministry of Ecology and Environment the People's Republic of China
85 (<http://www.mee.gov.cn/>). In addition, we categorized air pollution levels with the surface $PM_{2.5}$
86 concentrations based on the National Ambient Air Quality Standards of China (HJ633-2012) released by
87 the Ministry of Ecology and Environment in 2012 as shown in Table 1.

88 We also used the monthly air temperature of surface observation data during 1960-2014 from 58
89 meteorological observation stations in the plateau area with an altitude above 3000 meters, which were
90 archived from the China Meteorological Information Center (<http://data.cma.cn/>).

91 Furthermore, the L-band sounding 'seconds-level' data of Beijing from 2010 to 2019 to were used to
92 calculate the height of ABL (Liu and Liang, 2010). The height of ABL top is characterized by the L-band
93 sounding observations at 20:00 (local time is used for this paper). The L-band sounding 'seconds-level'
94 data has been undergone the quality control before analysis (Zhu et al., 2018), and interpolation was
95 implemented in a vertical direction at an interval of 2 hPa. The L-band detection data provided by the
96 China Meteorological Information Center (<http://data.cma.cn/>) contains several automatic observation

97 meteorological elements with time resolution of 1.2 s and vertical resolution of 8 m. More detail
 98 information can be found in Li et al. (2009) and Cai et al. (2014).

99 **Table 1. Air pollution degrees categorized with surface PM_{2.5} concentrations**

Air pollution degrees	PM _{2.5} concentration ranges
‘less-serious’ pollution	$75 \mu\text{g}\cdot\text{m}^{-3} < \text{PM}_{2.5} \leq 115 \mu\text{g}\cdot\text{m}^{-3}$
‘serious’ pollution	$115 \mu\text{g}\cdot\text{m}^{-3} < \text{PM}_{2.5} \leq 150 \mu\text{g}\cdot\text{m}^{-3}$
‘more-serious’ pollution	$150 \mu\text{g}\cdot\text{m}^{-3} < \text{PM}_{2.5} \leq 250 \mu\text{g}\cdot\text{m}^{-3}$
‘most-serious’ pollution	$\text{PM}_{2.5} > 250 \mu\text{g}\cdot\text{m}^{-3}$

100

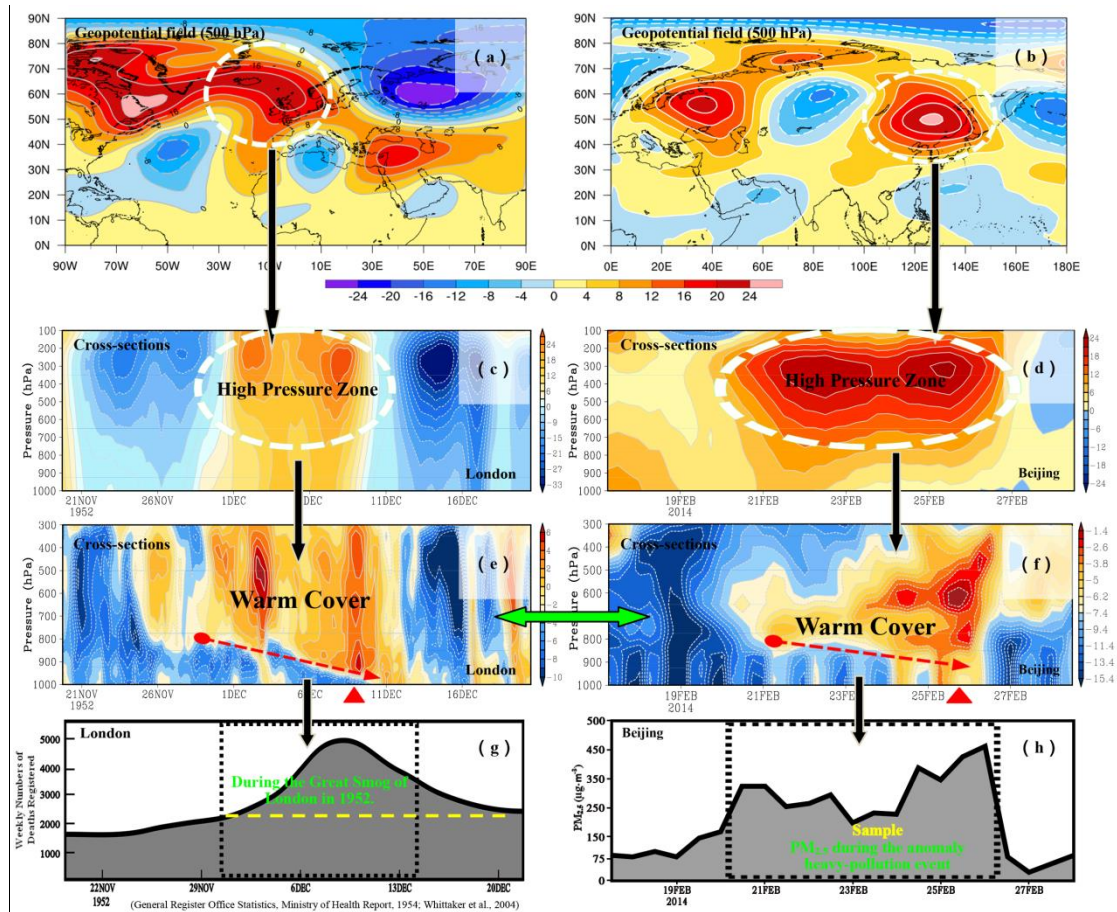
101 **3 Results**

102 **3.1 A precursory ‘strong signal’ of ‘warm cover’ in the middle troposphere**

103 In February 2014, a rarely persistent air pollution weather process occurred in EC with severe air pollution
 104 in more than 50 cities, with an impact area of 2.07 million km². In the Beijing area during February 20–26,
 105 2014 the regional average PM_{2.5} concentration exceed the ‘most-serious’ air pollution level, and with a
 106 peak value of up to 456 μg·m⁻³. In addition, the Great Smog of London in 1952 was attributed to the
 107 long-lasting and heavy haze pollution under the influence of certain weather systems (Whittaker et al.,
 108 2004). To find the precursory ‘strong signals’ hidden in meteorology for heavy air pollution events, we
 109 retrieved the three-dimensional atmospheric dynamic and thermal structures during December in 1952 as
 110 well as February in 2014 by analyzing vertical anomalies of meteorology. There were high-pressure
 111 systems moved to London as well as Beijing and stagnated over both areas at 500 hPa geopotential
 112 height anomalies, as shown in Figs. 1a and 1b. During the heavy air pollution events, a high-pressure
 113 system over London as well as Beijing gradually strengthened (Figs. 1c and 1d), and the middle
 114 troposphere was characterized by a ‘warm cover’ with ‘upper warming and bottom cooling’ anomalies in
 115 vertical structure of air temperature (Figs. 1e and 1f).

116 By comparing Figs. 1a and 1b, we found that two persistent heavy air pollution events occurred during

117 the maintenance stage of stable high pressure system. During stagnation of the blocking high pressure
118 system, the strength of the center of the geopotential height anomalies in the stable maintenance region of
119 the blocking exhibited a synchronous response to the ‘warm cover’ above areas (Figs. 1c–1f). It can be seen
120 that the local atmospheric thermal structure is significantly modulated by the persistent large-scale
121 anomalous circulation. The ‘subsidence-induced air temperature inversion’ effect of the blocking high
122 pressure system continuously strengthened the ‘warm cover’ structure in the middle troposphere, which
123 suppressed the vertical diffusion capacity in the atmosphere (Cai et al., 2020). Moreover, it was obvious
124 that ‘strong signals’ arising from the thick ‘warm cover’ persisted during the abnormal air-pollution episode
125 during December 5–9, 1952 in London as well as February 21–26, 2014 in Beijing. It is worth pointing out
126 that the bottom edge of ‘warm cover’ in the free troposphere declined day-by-day. During the heavy
127 pollution incident, the ‘warm cover’ dropped to 900 hPa (Figs. 1g and 1h). The above analysis shows that
128 in the ABL over London during December 5–9, 1952 and Beijing during February 21–26, 2014, the
129 inversion layer height decreased, which made the ABL structure stable for accumulation of air pollutants.
130 The deep ‘warm cover’ structures in the middle troposphere acted as a precursory ‘strong signal’ of the
131 Great Smog of London and Beijing’s heavy air pollution.



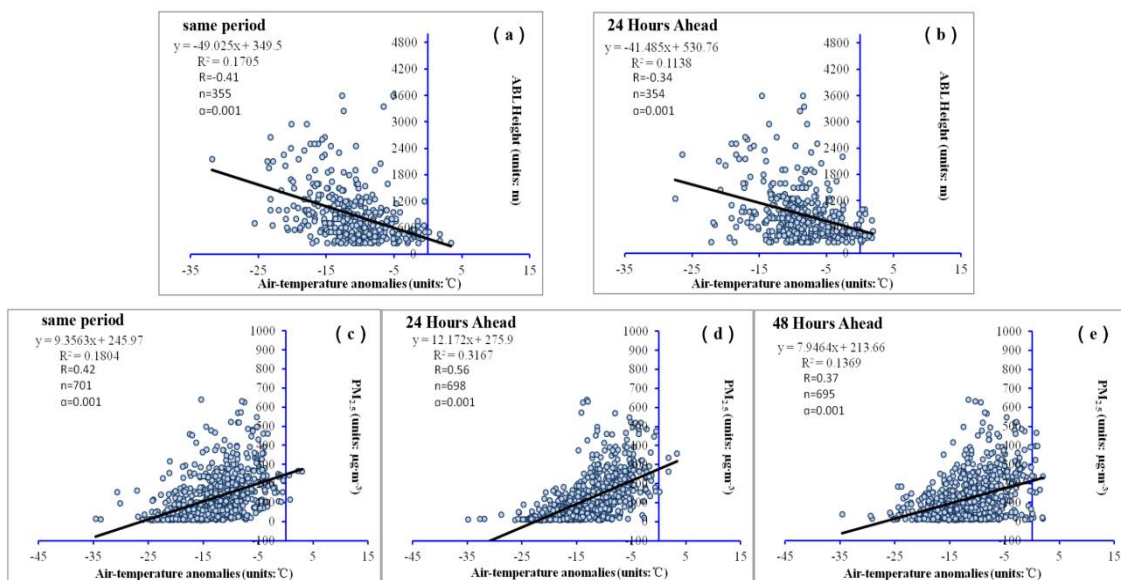
132
 133 **Figure 1.** Dynamical and thermodynamical structures and air pollution variations: (a) geopotential height anomalies (unit:
 134 dagpm) at 500 hPa during December 5–9, 1952 for the Great Smog of London, (b) the same as (a) but during February 21–26,
 135 2014. (c) Time-vertical cross-sections of the geopotential height anomalies (unit: dagpm) in the high pressure area (50–70 °N;
 136 20 ° W–10 ° E) during November 20 to December 20, 1952, (d) the same as (c) but in the high pressure area (40–63 ° N;
 137 115–138 ° E) during February 17–28, 2014. (e) Time-vertical cross-sections of air temperature anomalies (unit: °C) over
 138 London (the Red dotted arrow shows the bottom edge of the ‘warm cover’ during the Great Smog in London) during
 139 November 20 to December 20, 1952, (f) the same as (e) but during the heavy pollution in February 2014 over Beijing. (g)
 140 Weekly death rate in London prior to, during and after the 1952 pollution episode (General Register Office Statistics,
 141 Ministry of Health Report, 1954; Whittaker et al., 2004). (h) The variation of surface PM_{2.5} concentrations (units: $\mu\text{g}\cdot\text{m}^{-3}$)
 142 during the heavy pollution in February 2014 over Beijing.

143

144 3.2 Effect of ‘Warm Cover’ in the free troposphere on ABL and surface PM_{2.5} variations

145 During five heavy air pollution episodes over Beijing in December 2015 and 2016 the vertical structures of
 146 air temperature anomalies presented the ‘warm cover’ structure in the free troposphere (see Fig. S1).

147 During winter 2014–2017, Figs. 2a and 2b demonstrated the significant negative correlations between the
 148 height of the ABL and air temperature anomalies over same period and 24 hours ahead in Beijing, and the
 149 correlation coefficients were 0.41 and 0.34 (99.9 % confidence level), reflecting that the ‘warm cover’
 150 structure hidden in the middle troposphere with significant ‘strong-signal’ features is of persistent
 151 premonitory significance for the heavy pollution episodes. Figures 2c–2e presented the significant
 152 positive correlations between PM_{2.5} concentrations and air temperature anomalies over same period and 24,
 153 48 hours ahead in Beijing, and the correlation coefficients were 0.42, 0.56 and 0.37 (99.9 % confidence
 154 level). Based on the above mentioned results, air temperature anomalies over 24 and 48 hours ahead
 155 could also be reflected that ‘warm cover’ hidden in the middle troposphere could be regarded as the
 156 precursory ‘strong-signal’ for air pollution change. Furthermore, such a ‘stable’ structure also restricted
 157 the vertical transport of moist air from the lower to the middle troposphere for forming secondary aerosols,
 158 which could dominate PM_{2.5} concentrations in air pollution over China (Huang et al., 2014; Tan et al.,
 159 2015).



160
 161 **Figure 2.** The correlations between ABL height and air temperature anomalies in Beijing during winter 2014–2017, (a) same
 162 period, at 800 hPa; (b) 24 hours ahead, at 650 hPa. The correlations between PM_{2.5} concentration and air temperature

163 anomalies in Beijing during winter 2014–2017, (c) same period, at 850 hPa; (d) 24 hours ahead, at 800 hPa; (e) 48 hours
164 ahead, at 724 hPa.

165

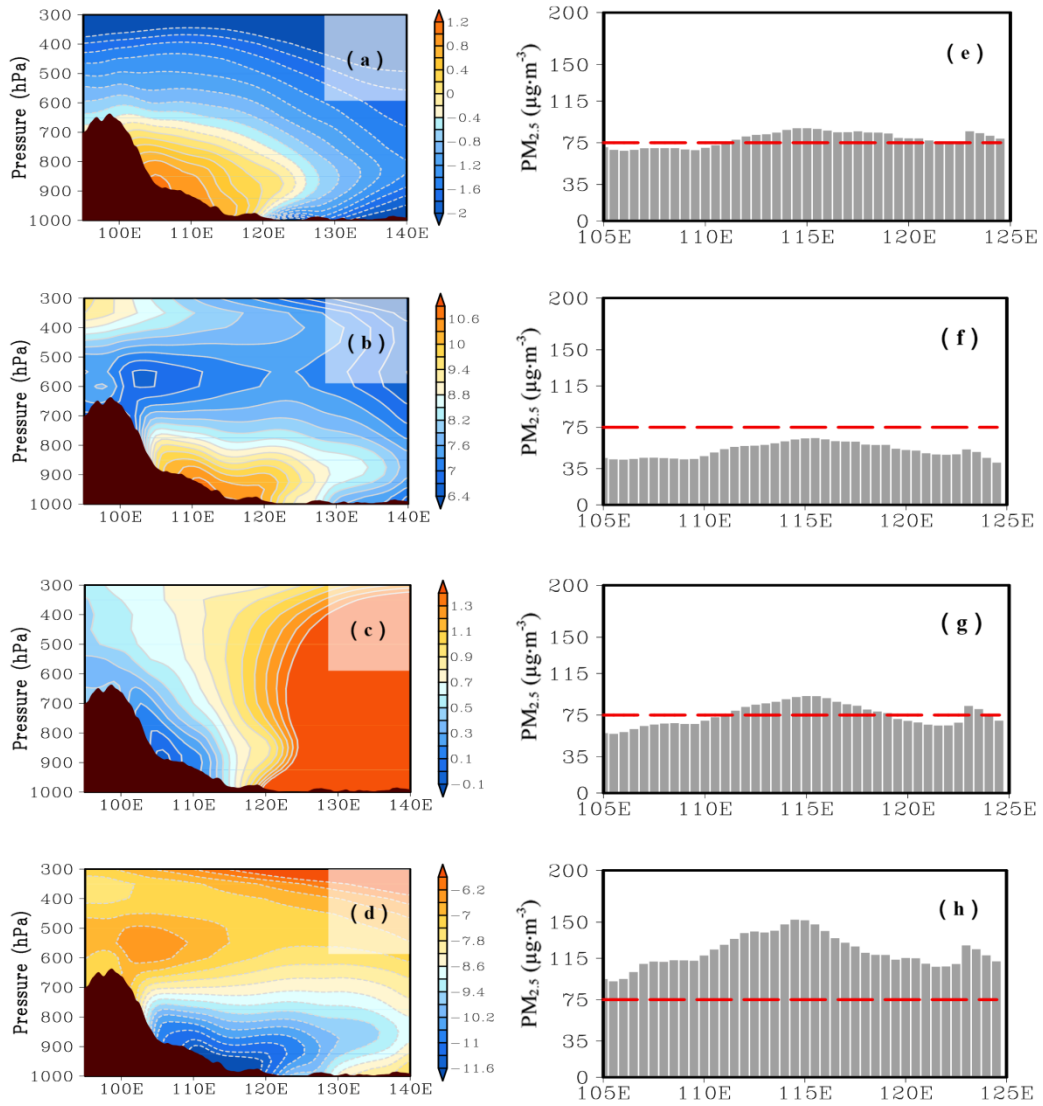
166 **3.3 Changes of the ‘warm cover’ structure in the middle troposphere**

167 The ‘warm cover’ structure of air temperature anomalies in the middle troposphere indicated the
168 intensification of heavy air pollution. The ‘warm cover’ structure is a precursory ‘strong signal’ for the
169 frequent occurrence of regional haze events. The air pollution in EC exhibited the significant seasonal
170 variations. Our study revealed that existed seasonal differences of the thermal structures in the atmosphere
171 over EC. In spring (Figs. 3a and 3e) and summer (Figs. 3b and 3f), the middle troposphere was
172 characterized by a ‘upper cooling and bottom warming’ vertical structure for less air pollution. When the
173 autumn (Figs. 3c and 3g) and winter (Figs. 3d and 3h) arrived, the middle troposphere was characterized by
174 a ‘upper warming and bottom cooling’ vertical structure, which intensified the air pollution. In autumn,
175 atmospheric thermal structure over EC was marked with a transition between summer and winter (Fig. 3c).
176 The atmosphere condition reversed in winter, a large-scale anomalous air temperature pattern of ‘upper
177 warming and bottom cooling’ in the middle troposphere appeared from the plateau to downstream EC
178 region and even the entire East Asian region (Fig. 3d). The structure of ‘warm cover’ in winter was much
179 stronger than that in autumn, and its height of the former was much lower than that of the latter. Therefore,
180 the intensity of air pollution over EC during winter is significantly higher than other seasons (Fig. 3h).

181 From the perspective of interdecadal variations, our study revealed a close relationship between the
182 frequent occurrence of haze events in EC and the atmospheric thermal structure in the eastern Tibetan
183 Plateau (TP). Furthermore, the thermal structures of the troposphere exhibited the distinct interdecadal
184 variations (Figs. 4a-4c). A cooling structure was identified in the wintertime air temperature anomalies over
185 the east region of TP during 1961–1980 (Fig. 4a); the upper level of the eastern TP during 1981–2000

186 showed a ‘upper cooling and bottom warming’ vertical structure (Fig. 4b). The interdecadal changes of
187 vertical structure reversed during 2001–2018 with a significant ‘warm cover’ (Fig. 4c). The years of 2001–
188 2018 witnessed the highest frequency of haze days (Fig. 4f), and 1981–2000 saw a middle-level occurrence
189 of haze days (Fig. 4e), while the lowest frequency of haze days occurred during 1961–1980 (Fig. 4d).

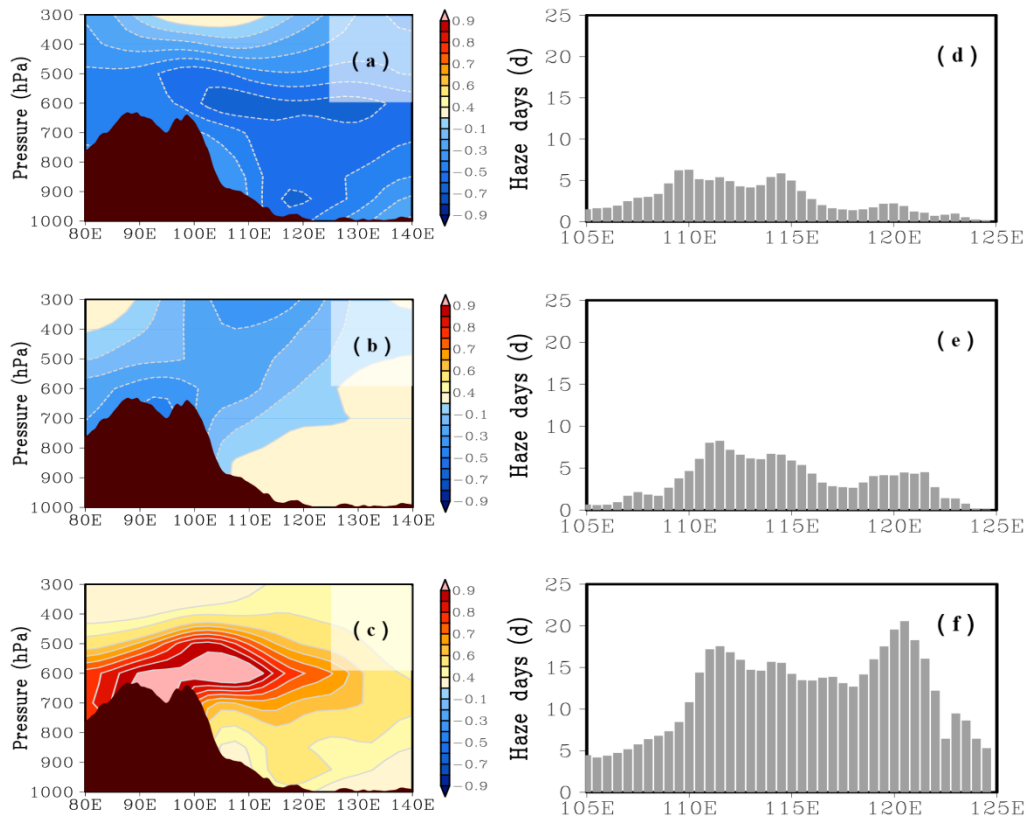
190 The concept of variations of the tropospheric ‘warm cover’ has been proposed in this work. Under the
191 background of climate change, it is worth considering whether the variational tendency of the structure of
192 the plateau’s heat source induces variations of the tropospheric thermal structure in downstream areas of the
193 Plateau, leading to the interdecadal variations of the frequency of haze events seen in Eastern China since
194 the 21th century. Thermal anomalies of the TP also play an important role in the variations of the frequency
195 of haze events in EC apart from the anthropogenic pollutant emission related to the rapid industrialization
196 of China. The observational and modeling studies have demonstrated that the interannual variations in the
197 thermal forcing of TP are positively correlated with the incidences of wintertime haze over EC (Xu et al.,
198 2016). The TP induced changes in atmospheric circulation, increasing atmospheric stability and driving
199 frequent haze events in EC (Xu et al., 2016). In this study, the data analysis concerning the interannual
200 variations of the TP’s apparent heat source and air temperature in wintertime at the TP with the altitudes
201 above 3000 meters showed that since the 1960s the heat source in areas vulnerable to TP climate change
202 strengthen continuously as the surface temperature increased (Fig. 5a). Furthermore, the TP’s apparent heat
203 and air temperature of the middle troposphere over EC presented the significant positive correlation passing
204 (90 % confidence level), which is similar to ‘warm cover’ structures (Fig. 5b). Therefore, we considered
205 that the ‘warm cover’ change in the middle troposphere over EC was closely related to TP’s apparent heat
206 and the surface temperature. The TP induced changes in thermodynamic structure of atmospheric provided
207 favorable climatic backgrounds driving air pollution events in EC.



208

209 **Figure 3.** Vertical cross sections of (a-d) air temperature anomalies (unit: °C) and (e-h) the $PM_{2.5}$ concentrations (unit: $\mu\text{g}\cdot\text{m}^{-3}$)

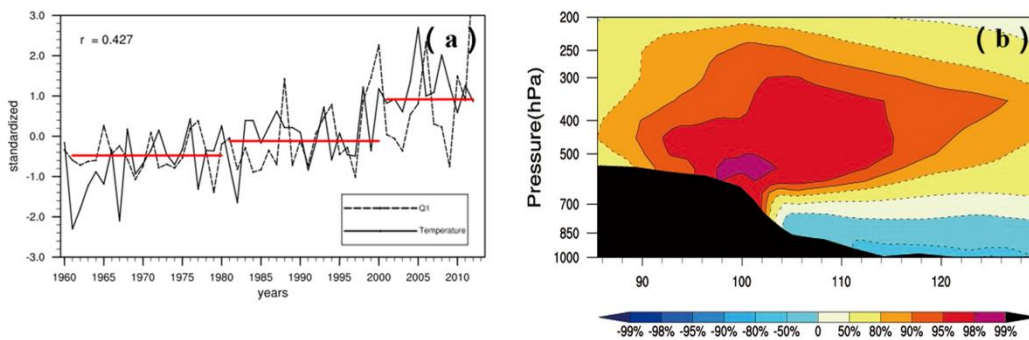
210 averaged along 25-40 °N in spring (a, e), summer (b, f), autumn (c, g), winter (d, h) from 2013 to 2018.



211

212 **Figure 4.** Vertical cross sections of (a-c) air temperature anomalies (unit: °C) and (d-f) the number of haze days averaged
 213 along 25-40°N in winter during 1961-1980 (a, d), 1981-2000 (b, e) and 2001-2018 (c, f).

214



215

216 **Figure 5.** (a) Interannual variations of TP's apparent heat source (Q_1) and air temperature of meteorological stations in the TP
 217 with the altitudes above 3000 meters in the winters during 1960-2014; (b) Vertical cross sections of the correlations between
 218 TP's apparent heat (Q_1) and air temperature latitude-averaged along 30-35°N in the winters during 1960-2014.

219

220 4 Conclusions and discussion

221 Based on the study of the Great Smog of London in 1952 and Beijing's heavy air pollution in 2014, as well

222 as PM_{2.5} pollution over EC, the anomalous ‘warm cover’ in the middle troposphere was identified as a
223 precursory ‘strong signal’ for severe air pollution events, which could be attributed to climate change. A
224 stable thermal structure in the middle troposphere, i.e. a ‘warm cover’, suppressed the ABL development,
225 which was a key ‘inducement’ for the accumulation of air pollutants in the ambient atmosphere.

226 From the perspective of the thermal vertical structure in the troposphere, the abnormal vertical
227 structure in the troposphere during heavy air pollution were understood in this study. The thermal structure
228 formed by the conventional decline rate of atmospheric air temperature often ‘covers up’ the anomalous
229 ‘strong signal’ of the troposphere in air pollution process, such as the abnormal stable structure with the
230 middle warm and bottom cold in the troposphere with air temperature anomalies. The ‘strong signal’ of the
231 ‘warm cover’ of air temperature anomalies in the middle troposphere during heavy air pollution can be
232 described by the method of statistical comprehensive diagnosis analysis.

233 A large-scale anomalous air temperature pattern of ‘upper warming and bottom cooling’ in the
234 troposphere appeared from the TP to the downstream EC region and even the entire East Asian region. The
235 frequent haze pollution events in EC since the start of the 21st century happens to be within a significant
236 positive phase in the interdecadal variations of ‘warm cover’ in the middle troposphere. A close relationship
237 between the TP’s heat and the thermal structure in the atmosphere in EC and even the entire East Asian
238 region reflected an important role of TP’s thermal forcing in environment change over China.

239

240 *Data availability.* The monthly NCEP/NCAR reanalysis data of meteorology are collected from the U.S.
241 National Center for Environmental Protection (NCEP, <https://www.esrl.noaa.gov/>); the daily and monthly
242 ERA-Interim reanalysis data of meteorology are collected from the European Center for Medium-range
243 Weather Forecasts (ECMWF, <https://www.ecmwf.int/>); the hourly PM_{2.5} concentration data are collected

244 from the national air quality monitoring network operated by the Ministry of Ecology and Environment the
245 People's Republic of China (<http://www.mee.gov.cn/>); the air temperature of surface observation data and
246 L-band sounding data are obtained from the China Meteorological Information Center (<http://data.cma.cn/>).
247 All data presented in this paper are available upon request to the corresponding author (Wenyue Cai,
248 caiwy@cma.gov.cn).

249
250 *Author contributions.* XDX and WYC designed the study. XDX, WYC and TLZ performed the research.
251 WYC performed the statistical analyses. XDX, WYC and TLZ wrote the initial paper. TLZ, XFQ, WHZ,
252 CS, PY, CZW and FG contributed to subsequent revisions.

253
254 *Competing interests.* The authors declare that they have no conflict of interest.

255
256 *Acknowledgements.* This study is supported by the Atmospheric Pollution Control of the Prime Minister
257 Fund (DQGG0104), the National Natural Science Foundation of China (91644223) and the Second Tibet
258 Plateau Scientific Expedition and Research program (STEP, 2019QZKK0105).

259
260 *Financial support.* This research has been supported by the Atmospheric Pollution Control of the Prime
261 Minister Fund (DQGG0104), the National Natural Science Foundation of China (91644223) and the
262 Second Tibet Plateau Scientific Expedition and Research program (STEP, 2019QZKK0105).

263
264 **References**

265 Cai, M., OU, J. J., Zhou, Y. Q., Yang Q., and Cai, Z. X.: Discriminating cloud area by using L-band
266 sounding data (in Chinese), *Chin. J. Atmos. Sci.*, 38, 213–222,
267 <https://doi.org/10.3878/j.issn.1006-9895.2013.12193>, 2014.

268 Cai, W. Y., Xu, X. D., Cheng, X. H., Wei, F. Y., Qiu, X. F., and Zhu, W. H.: Impact of “blocking” structure
269 in the troposphere on the wintertime persistent heavy air pollution in northern China, *Sci. Total*
270 *Environ.*, 741, 140325, <https://doi.org/10.1016/j.scitotenv.2020.140325>, 2020.

271 Cheng, Y. F., Zheng, G. J., Wei, C., Mu, Q., Zheng, B., Wang, Z. B., Gao, M., Zhang, Q., He, K. B.,
272 Carmichael, G., Poschl, U., and Su, H.: Reactive nitrogen chemistry in aerosol water as a source of
273 sulfate during haze events in China, *Sci. Adv.*, 2, e1601530, <https://doi.org/10.1126/sciadv.1601530>,
274 2016.

275 China Ministry of Environmental Protection: Technical Regulation on Ambient Air Quality Index (On Trial)
276 (HJ633-2012), China Environmental Science Press, Beijing, China, 2012.

277 Ding, Y. H. and Liu, Y. J.: Analysis of long-term variations of fog and haze in China in recent 50 years and
278 their relations with atmospheric humidity, *Sci. China Earth Sci.*, 57, 36-46,
279 <https://doi.org/10.1007/s11430-013-4792-1>, 2014.

280 Huang, R. J., Zhang, Y., Bozzetti, C., Ho, K. F., Cao, J. J., Han, Y. M., Daellenbach, K. R., Slowik, J. G.,
281 Platt, S. M., Canonaco, F., Zotter, P., Wolf, R., Pieber, S. M., Bruns, E. A., Crippa, M., Ciarelli, G.,
282 Piazzalunga, A., Schwikowski, M., Abbaszade, G., Schnelle-Kreis, J., Zimmermann, R., An, Z. S.,
283 Szidat, S., Baltensperger, U., Haddad, I. E., 11, and Prevot, A-S. H.: High secondary aerosol
284 contribution to particulate pollution during haze events in China, *Nature*, 514, 218–222,
285 <https://doi.org/10.1038/nature13774>, 2014.

286 Li, W., Li, F., Zhao, Z. Q., Liu, F. Q., Li, B., Li, H.: L-Band Meteorological Observation System
287 Construction Technology Assessment Report (in Chinese), China Meteorological Press, Beijing, China,
288 2009.

289 Liu, S. Y. and Liang, Z. X.: Observed diurnal cycle climatology of planetary boundary layer height, *J.*
290 *Climate*, 23, 5790-5809, <https://doi.org/10.1175/2010JCLI3552.1>, 2010.

291 Miao, Y. C., Li, J., Miao, S. G., Che, H. Z., Wang, Y. Q., Zhang, X. Y., Zhu, R., and Liu, S. H.: Interaction
292 Between Planetary Boundary Layer and PM_{2.5} Pollution in Megacities in China: a Review. *Curr. Pollut.*
293 *Rep.*, 5, 261–271, <https://doi.org/10.1007/s40726-019-00124-5>, 2019.

294 Quan, J. N., Gao, Y., Zhang, Q., Tie, X. X., Cao, J. J., Han, S. Q., Meng, J. W., Chen, P. F., and Zhao, D. L.:
295 Evolution of planetary boundary layer under different weather conditions, and its impact on aerosol
296 concentrations, *Particuology*, 11(1), 34-40, <https://doi.org/10.1016/j.partic.2012.04.005>, 2013.

297 Quan, J. N., Xu, X. D., Jia, X. C., Liu, S. H., Miao, S. G., Xin, J. Y., Hu, F., Wang, Z. F., Fan, S. J., Zhang,
298 H. S., Mu, Y. J., Dou, Y. W., and Cheng, Z.: Multi-scale processes in severe haze events in China and
299 their interactions with aerosols: Mechanisms and progresses (in Chinese). *Chin. Sci. Bull.*, 65, 810–
300 824, <https://doi.org/10.1360/TB-2019-0197>, 2020.

301 State Council of the People’s Republic of China: Notice of the General Office of the State Council on
302 Issuing the Air Pollution Prevention and Control Action Plan, State Council of the People’s Republic
303 of China website. Available at: http://www.gov.cn/zwgk/2013-09/12/content_2486773.htm, 2013.

304 State Council of the People’s Republic of China: Notice of the General Office of the State Council on
305 Issuing the Air Pollution Prevention and Control Action Plan, State Council of the People’s Republic
306 of China website. Available at: http://www.gov.cn/zhengce/content/2018-07/03/content_5303158.htm.
307 2018.

308 Tan, C. H., Zhao, T. L., Cui, C. G., Luo, B. L., and Bai, Y. Q.: Characterization of haze pollution over
309 Central China during the past 50 years, *Science in China (in Chinese)*, *China Environ. Sci.*, 35, 2272–
310 2280, 2015.

311 Tang, G. Q., Zhang, J. Q., Zhu, X. W., Tao, S., Munkel, C., Hu, B., Schaefer, K., Liu, Z. R., Zhang, J. K.,
312 Wang, L. L., Xin, J. Y., Schaefer, P., and Wang, Y. S.: Mixing layer height and its implications for air
313 pollution over Beijing, China, *Atmos. Chem. Phys.*, 16, 2459–2475,
314 <https://doi.org/10.5194/acp-16-2459-2016>, 2016.

315 Tie, X. X. and Cao, J. J.: Aerosol pollutions in eastern China: Present and future impacts on environment,
316 *Particuology*, 7, 426–431, <https://doi.org/10.1016/j.partic.2009.09.003>, 2009.

317 Wang, G. H., Zhang, R. Y., Gomez, M. E., Yang, L. X., Zamora, M. L., Hu, M., Lin, Y., Peng, J. F., Guo, S.,

318 Meng, J. J., Li, J. J., Cheng, C. L., Hu, T. F., Ren, Y. Q., Wang, Y. S., Gao, J., Cao, J. J., An, Z. S.,
319 Zhou, W. J., Li, G. H., Wang, J. Y., Tian, P. F., Marrero-Ortiz, W., Secretst, J., Du, Z. F., Zheng, J.,
320 Shang, D. J., Zeng, L. M., Shao, M., Wang, W. G., Huang, Y., Wang, Y., Zhu, Y. J., Li, Y. X., Hu, J. X.,
321 Pan, B., Cai, L., Cheng, Y. T., Ji, Y. M., Zhang, F., Rosenfeld, D., Liss, P. S., Duce, R. A., Kolb, C. E.,
322 and Molina, M. J.: Persistent sulfate formation from London Fog to Chinese Haze, *P. Natl. Acad. Sci.*,
323 113, 13630–13635, <https://doi.org/10.1073/pnas.1616540113>, 2016.

324 Wang, H., Li, J. H., Peng, Y., Zhang, M., Che, H. Z., and Zhang, X. Y.: The impacts of the meteorology
325 features on PM_{2.5} levels during a severe haze episode in central-east China, *Atmospheric Environ.*, 197,
326 177–189, <https://doi.org/10.1016/j.atmosenv.2018.10.001>, 2019.

327 Wang, H., Xue, M., Zhang, X. Y., Liu, H. L., Zhou, C. H., Tan, S. C., Che, H. Z., Chen, B., and Li, T.:
328 Mesoscale modeling study of the interactions between aerosols and PBL meteorology during a haze
329 episode in Jing–Jin–Ji (China) and its nearby surrounding region – Part 1: Aerosol distributions and
330 meteorological features, *Atmos. Chem. Phys.*, 15, 3257–3275,
331 <https://doi.org/10.5194/acp-15-3257-2015>, 2015.

332 Wang, J. J., Zhang, M. G., Bai, X. L., Tan, H. J., Li, S., Liu, J. P., Zhang, R., Wolters, M. A., Qin, X. Y.,
333 Zhang, M. M., Lin, H. M., Li, Y. N., Li, J., and Chen, L. Q.: Large-scale transport of PM_{2.5} in the
334 lower troposphere during winter cold surges in China, *Sci. Rep.*, 7, 13238,
335 <https://doi.org/10.1038/s41598-017-13217-2>, 2017.

336 Wang, Y. S., Li, W. J., Gao, W. K., Liu, Z. R., Tian, S. L., Shen, R. R., Ji, D. S., Wang, S., Wang, L. L.,
337 Tang, G. Q., Song, T., Cheng, M. T., Wang, G. H., Gong, Z. Y., Hao, J. M., and Zhang, Y. H.: Trends in
338 particulate matter and its chemical compositions in China from 2013–2017. *Sci. China Earth Sci.*, 62:
339 1857–1871, <https://doi.org/10.1007/s11430-018-9373-1>, 2019.

340 Whittaker, A., Berube, K., Jones, T., Maynard, R., Richards, R.: Killer smog of London, 50 years on:
341 particle properties and oxidative capacity, *Sci. Total Environ.*, 334–335, 435–445,
342 <https://doi.org/10.1016/j.scitotenv.2004.04.047>, 2004.

343 Xu, X. D., Zhao, T. L., Liu, F., Gong, S. L., Kristovich, D., Lu, C., Guo, Y., Cheng, X. H., Wang, Y. J., and
344 Ding, G.: Climate modulation of the Tibetan Plateau on haze in China, *Atmos. Chem. Phys.*, 16, 1365–
345 1375, <https://doi.org/10.5194/acp-16-1365-2016>, 2016.

346 Yim, S.-Y., Wang, B., Liu, J., and Wu, Z. W.: A comparison of regional monsoon variability using monsoon
347 indices, *Clim. Dynam.*, 43, 1423–1437, <https://doi.org/10.1007/s00382-013-1956-9>, 2014.

348 Zhang, X. Y., Wang, J. Z., Wang, Y. Q., Liu, H. L., Sun, J. Y., and Zhang, Y. M.: Changes in chemical
349 components of aerosol particles in different haze regions in China from 2006 to 2013 and contribution
350 of meteorological factors, *Atmos. Chem. Phys.*, 15, 12935–12952,
351 <https://doi.org/10.5194/acp-15-12935-2015>, 2015.

352 Zhu, W. H., Xu, X. D., Zheng, J., Yan, P., Wang, Y. J., and Cai, W. Y.: The characteristics of abnormal
353 wintertime pollution events in the Jing-Jin-Ji region and its relationships with meteorological factors,
354 *Sci. Total Environ.*, 626, 887-898, <https://doi.org/10.1016/j.scitotenv.2018.01.083>, 2018.